IRON ISOTOPE FRACTIONATION DURING ASTEROIDAL CORE CRYSTALLIZATION. Peng Ni[1], Nancy L. Chabot[2], Caillin J. Ryan[2], and Anat Shahar[1]. [1]Geophysical Laboratory, Carnegie Insititution for Science, 5251 Broad Branch Rd. NW, Washington, DC 20015, USA. [2]Johns Hopkins University Applied Physics Laboratory, 11100 Johns Hopkins Rd., Laurel, MD 20723, USA. pni@carnegiescience.edu

Introduction: Stable isotope systems are powerful tools in understanding the formation and evolution of planetary bodies, because isotope fractionations have the potential to record evidence of the physical and chemical processes that occurred during planetary accretion and differentiation.

Recent developments in Fe isotope analyses enable precise measurements of Fe isotopic compositions in various types of planetary samples, which show significant variations [1-6]. For example, terrestrial mantle peridotites have an average δ^{57}Fe composition of 0.040 ± 0.040‰ [1], indistinguishable from the chondritic δ^{57}Fe of ~0‰ [2], but the δ^{57}Fe for the mid-ocean basalts (MORB) is significantly heavier (0.151 ± 0.010‰) [1,2,3]. Basaltic meteorite samples from Mars and Vesta, on the other hand, have Fe isotopic compositions that are within analyrical error compared to the chondritic value [4]. Besides the planetary silicate samples, magmatic iron meteorites, which are thought to be from the cores of asteroidal bodies, also show heavy Fe isotopes relative to the chondrites, with a wide range of variation (~0.4 ‰, Fig. 1) [5,6,7]. The causes of the heavier Fe isotopes and their large variations in iron meteorites are poorly understood. To better understand Fe isotope fractionation in iron meteorites, we conducted solid-liquid metal equilibrium experiments to determine Fe isotope fractionation factors between the two phases, and explored the effect of asteroidal core crystallization on their Fe isotope evolution.

Experimental and Analytical Methods: All solid-liquid metal equilibrium experiments were conducted at the Johns Hopkins University Applied Physics Laboratory using established techniques [e.g. 8]. Starting mixtures of commercially purchased Fe, FeS, and Ni powders, doped with 0.3 wt% each of Ru, Os, and W, were sealed in evacuated silica tubes for the experiments. The experiments were conducted using a 0.1 MPa Deltech vertical furnace at 1260 to 1470 ºC for durations of 1 to 7 days. All the experiments were spiked with ^{54}Fe to confirm isotopic equilibrium with the three-isotope exchange method. Two sets of time-series experiments were also conducted at 1260 and 1325 ºC for 2 to 7 days and 1 to 3 days to ensure that isotopic equilibrium was achieved.

Experiment run products were cut and set in epoxy, and then polished with alumina powder. Major element compositions were measured using a JEOL 8530F electron microprobe at the Carnegie Institution for Science. A set of pure element standards and a NiS standard were used for standardization. A large beam size of 100 µm was employeed to overcome chemical heterogeneities caused by the quench textures, which are common for the liquid metal phase in the Fe-Ni-S system [e.g. 8].

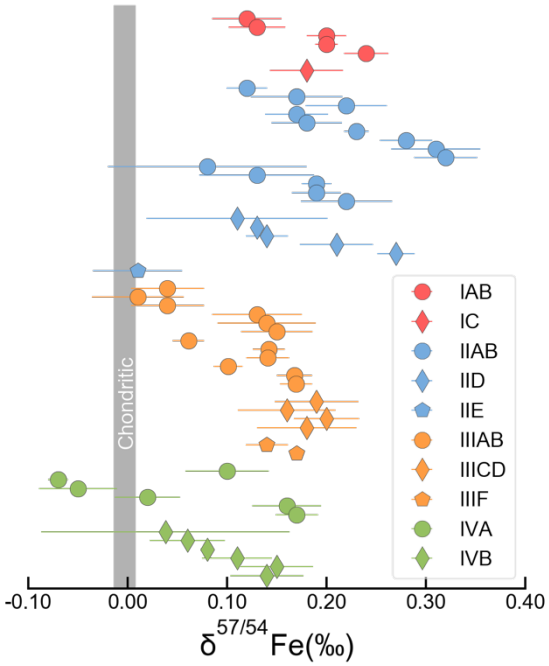

Figure 1. δ^{57}Fe measurements for iron meteorites [5,6,7] are heavier than chondrites [2] and vary significantly.

Liquid and solid metal phases were sampled for Fe isotope analyses by a Newwave micromill loaded with tungsten carbide drill bits that are 300 to 700 µm in diameter. A drop of mili-Q water was placed on the sample to collect the drilled particles. The drilled particles were subsequently transferred to a Teflon beaker by repeatedly pipetting mili-Q water to and from the drilled location. The sample surface was then cleaned by mili-Q water and compressed air to remove any remaining loose particles. The drilled samples were dissolved with concentrated acid on a hot plate, and purified by column chemistry for Fe isotope analyses following the short column method described in [2]. Iron isotopic compositions were determined using the Nu Plasma II at the Carnegie Institution for Science

under high resolution mode. Analyses were conducted using the sample-standard bracketing method to correct for instrument drift and the concentration of Fe in the analytical solution was 4 ppm.

Results: The final products of the 11 experiments all contain 8 to 11 wt% Ni in the liquid metal and 10 to 13 wt% Ni in the solid metal. Sulfur concentrations in the liquid metal for different experiments vary from 4.3 wt% to 26.8 wt%, depending on the experimental temperature.

All starting materials for the experiments were spiked with ^{54}Fe metal to test if the liquid and solid metal phases achieved isotopic equilibrium during the experiments. The consequent departure from the terrestrial mass-dependent fractionation line, as quantified by $\Delta^{56}Fe = \delta^{56}Fe - 0.67795 \times \delta^{57}Fe$, are from -0.15 to -3.41 ‰ for all the experiments. For each experiment, the $\Delta^{56}Fe$ values are found to be identical between the solid and liquid metal phases, indicating isotopic equilibrium during the experiments. Isotopic equilibrium is also supported by the two sets of time-series experiments at 1260 and 1325 ºC, which gave fractionation factors that are within analytical errors (Fig. 2).

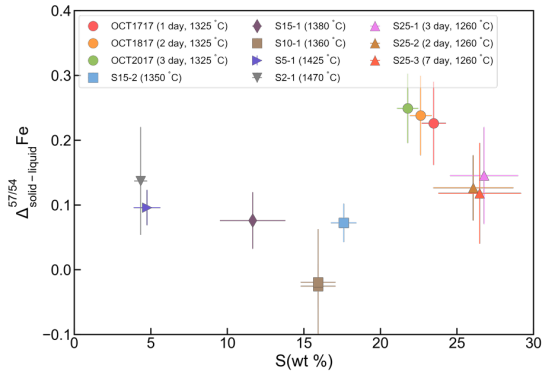

Figure 2. Preliminary data for δ^{57}Fe fractionation between solid and liquid metal phases. Error bars show 2σ standard error.

Our preliminary data are shown in Fig. 2. Most experiments show similar degrees of fractionation between the solid and liquid metal phases, with an average of $\Delta^{57}Fe_{sol\text{-}liq} = 0.11 \pm 0.06$ ‰. One experiment with 15 wt% S shows negligible fractionation between the solid-liquid metal, and the time-series experiments with 22 wt% S showing slightly higher fractionation (0.24 ‰), The similar fractionation factors across a wide range of sulfur concentrations indicate that sulfur content in the liquid metal phase has limited effects on Fe isotope fractionation during asteroidal core crystallization.

Discussion: With the experimentally determined fractionation factor between solid and liquid metal, we are now able to model the evolution of Fe isotopes in the crystallizing asteroidal core as it crystalizes. Among the different groups of iron meteorites studied in Fig. 1, IIIAB is the largest iron-meteorite group and it shows clear compositional trends indicating fractional crystallization of a metallic magma [9], making it the ideal candidate for us to model Fe isotope evolution during fractional crystallization.

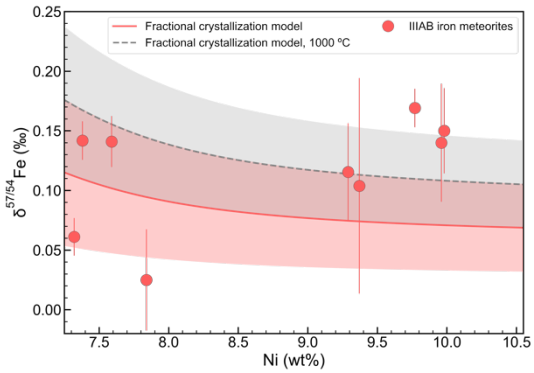

Figure 3. Modeled Fe isotopic evolution during core crystallization for the parent body of Group IIIAB iron meteorites. Iron meteorite data are from [5,6,7,9].

As plotted in Fig. 3, Ni concentration and δ^{57}Fe composition of the crystallized core are modeled following a well-established approach, assuming an initial bulk S content of 11 wt%, a Ni content of 7.2 wt%, and a chondritic $\delta^{57}Fe = 0$. The modeled trend (Fig. 3) shows well agreement with IIIAB iron meteorites with low degrees of crystallization (i.e. with < 8 wt% Ni). IIIAB iron meteorites with high degrees of crystallization have relatively high δ^{57}Fe values (~0.14‰), which might be due to an increase in the fractionation factor as the temperature decreases (Fig. 3, 1000 ºC model).

Overall, our experiments show significant equilibrium Fe isotope fractionation of ~0.11 ‰ between solid and liquid metal phases at 1470-1260 ºC, which could be a major mechanism that contributes to the enrichment of heavy Fe isotopes during asteroidal core crystallization as recorded by iron meteorites.

References: [1] Craddock P. R. et al. (2003) *EPSL, 365*, 63-76. [2] Craddock P. R. and Dauphas N. (2010) *Geostand. Geoanal. Res., 35*, 101-123. [3] Teng F. Z. et al. (2013) *GCA, 107*, 12-26. [4] Poitrasson F. et al. (2004) *EPSL, 223*, 253-266. [5] Poitrasson F. et al. (2005) *EPSL, 234*, 151-164. [6] Williams H. M. et al. (2006) *EPSL, 250*, 486-500. [7] Jordan M. K. et al. (2019) *GCA*, 246, 461-477. [8] Chabot N. L. et al. (2007) *Meteorit. Planet. Sci.*, *42*, 1735-1750. [9] Wasson J. T. (1999) *GCA*, *63*, 2875-2889.